SCIENTIFIC REPORTS

OPEN

SUBJECT AREAS:
BIOCHEMISTRY
BIOLOGICAL TECHNIQUES

Received
22 October 2013

Accepted
5 February 2014

Published
4 March 2014

Correspondence and requests for materials should be addressed to E.G. (ehudg@post.tau.ac.il)

Apoptosis induced by islet amyloid polypeptide soluble oligomers is neutralized by diabetes-associated specific antibodies

Yaron Bram, Anat Frydman-Marom, Inbal Yanai, Sharon Gilead, Ronit Shaltiel-Karyo, Nadav Amdursky & Ehud Gazit

Department of Molecular Microbiology and Biotechnology, Tel Aviv University, Ramat Aviv, Tel Aviv 69978, Israel.

Soluble oligomeric assemblies of amyloidal proteins appear to act as major pathological agents in several degenerative disorders. Isolation and characterization of these oligomers is a pivotal step towards determination of their pathological relevance. Here we describe the isolation of Type 2 diabetes-associated islet amyloid polypeptide soluble cytotoxic oligomers; these oligomers induced apoptosis in cultured pancreatic cells, permeated model lipid vesicles and interacted with cell membranes following complete internalization. Moreover, antibodies which specifically recognized these assemblies, but not monomers or amyloid fibrils, were exclusively identified in diabetic patients and were shown to neutralize the apoptotic effect induced by these oligomers. Our findings support the notion that human IAPP peptide can form highly toxic oligomers. The presence of antibodies identified in the serum of diabetic patients confirms the pathological relevance of the oligomers. In addition, the newly identified structural epitopes may also provide new mechanistic insights and a molecular target for future therapy.

The transition of proteins and peptides into highly-ordered amyloidal fibrilar structures is associated with major human disorders including Alzheimer's disease (AD), Parkinson's disease, Prion disorders and Type 2 diabetes (T2DM)[1]. Since the first observation of amyloid aggregates more than a century ago, it was suggested that insoluble amyloid deposits serve as major pathological agents in these disorders. This was based on histological observations indicating co-localization of tissue degeneration and amyloid accumulation. Moreover, further genetic data demonstrate the association between amyloid fibril formation and degenerative diseases, as aggregation-enhancing mutations in amyloidogenic proteins and polypeptides were linked to familial early-onset pathologies[2–4]. Nevertheless, the "amyloid dogma" has been challenged in the past years by several studies highlighting the discrepancy between the amount of amyloid deposits and disease severity[5–7]. In the case of Alzheimer's disease, a number of studies provided further evidence that the associated peptide amyloid-β (Aβ) oligomers are in fact significantly more cytotoxic than the mature amyloid fibrils[8–11]. In 2006 Ashe and coworkers demonstrated a clear correlation between cognitive reduction and the appearance of 56 kDa Aβ oligomers termed Aβ56* in Alzheimer's mice model[11]. Furthermore, the purification of Aβ56* and its intracranial reintroduction into the brain of wild type rats resulted in severe memory impairment. Ratnesh and coworkers have shown that different amyloidogenic polypeptides undergo supramolecular conformational changes in reconstituted membranes and form ion-channel-like structures with a similar morphology[12]. This led to the hypothesis suggesting that amyloid oligomers increase lipid bilayer conductance regardless of their sequence, whereas fibrils and soluble low-molecular weight species have no detectable effect on membranes[13]. Ramamoorthy and coworkers have shown that Aβ peptide disrupt biological membrane by a two step mechanism. First forming charge-selective pores and in a second phase this selectivity ceases and both positively and negatively charged molecules diffusion is observed across the membrane. This is consistent with a total loss of the physical integrity of the membrane[14]. These studies highlight a common structural motif observed in all types of amyloid oligomers. Given the structural similarities between the oligomers and the general cell toxicity observed, it is suggested that a similar toxic pathway prevalent in amyloid oligomers[15].

In 1901 two independent researchers described a phenomenon termed "islet hyalinization"[16,17] that occurred in association with diabetes mellitus (DM), especially in elderly population. However, the clinical importance of

these observations was not generally accepted since the phenomenon was not observed in all diabetes patients[18,19]. In 1986, 85 years after the first observation, the deposited material was successfully purified. Amino terminus amino acid sequencing revealed a novel peptide sharing sequence similarity with the calcitonin polypeptide family[20]. Further characterizations of the peptide from human and feline origins proved to be a 37 amino acid (a.a.) polypeptide denoted diabetes-associated peptide (DAP)[21], islet amyloid polypeptide (IAPP)[22], or amylin[23]. The relationship between the process of IAPP aggregation and the onset of Type 2 diabetes (T2DM) is not entirely understood. Nevertheless, over the years several studies have linked IAPP aggregation to the disease progression. It became clear that islet amyloidosis can affect less than 1% or up to 80% of islets of a diabetic individual[24]. The occurrence of islet amyloid deposits in non-diabetic subjects is low, less than 15% in non-diabetic individuals, but is relatively high in more than 90% of diabetic subjects at post-mortem[25]. Histological sections from T2DM patients have shown a positive correlation between amyloid aggregates and the reduction in β-cells mass of the pancreatic islets[26]. Moreover, missense mutation in IAPP gene has been identified in Asian population and was associated with early on-set and severity of T2DM[27].

The ex-vivo cytotoxicity of hIAPP was first described almost 20 years ago[28]. Human IAPP (hIAPP) but not rat IAPP (rIAPP) induced β-cell apoptosis. Moreover, cell membranes were observed to be decorated with hIAPP aggregates, and by causality the authors concluded that hIAPP fibrils induce apoptosis. However, subsequent studies challenged this observation and inclined towards soluble oligomers as the primary toxic species. Islet amyloids were also observed in non-diabetic individuals, particularly with elderly population[29], and are not present in all islets in patients with T2DM[30]. This was also observed in diabetic animal models as homozygous hIAPP transgenic mice developed severe diabetes due to a high rate of β cell apoptosis as early as at the age of 10 weeks[31]. However, extracellular islet amyloid was not yet observed in these mice during the rapid loss of β-cell from the age of 5–10 weeks. In obese hemizygous hIAPP mice, which develop diabetes at approximately 20 weeks of age, extensive islet amyloid formation does accrue, yet there is a poor correlation between the extent of amyloids and the frequency of β cell apoptosis[32]. *Ex-vivo* studies detected that the addition of hIAPP fibrilar aggregates did not increase the percentage of apoptotic cells. In contrast, freshly dissolved peptide samples added to cell culture induced apoptosis[33]. It has also been established that diabetic patients have elevated levels of the pro-inflammatory cytokines, especially interleukin 1β (IL-1β) which has a profound effect on the function of the cells[34]. Moreover, hIAPP oligomers, but not fibrils, were found as the cause for the activation of NLRP3 inflammasome which is a protein complex known to activate IL-1β[35].

All this data points towards an important role for IAPP oligomers in T2DM in general and β-cell damage in particular. The identification and isolation of soluble oligomers of IAPP which are involved in the pathology of the disease is of crucial importance for mechanistic understanding of the IAPP-induced degenerative process, as well as for the development of novel therapeutic agents that target the formation of such assemblies.

Results

Preparation of hIAPP oligomers. The identification and characterization of the various conformers of the self-assembly process is a crucial step towards the understanding of the linkage between the aggregation cascade and the observed pathology in different amyloid associated diseases. In spite of the extensive clinical importance of hIAPP self-assembly process in T2DM, the early stages of association are still not fully understood and soluble oligomers were not stabilized as distinctive entities. We aimed to characterize pathologically-relevant soluble assemblies of hIAPP, and their connection to the loss of β-cell mass in T2DM. As described above, we have searched for an experimental setup which will allow the observation of the restricted initial self-assembly products, prior to the appearance of large amyloid fibrilar structures, for a significant period.

Lyophilized hIAPP peptide was dissolved in 1,1,1,3,3,3-Hexafluoro-2-propanol (HFIP) to eliminate any pre-existing supramolecular structures. After evaporation the peptide was resuspended in 0.2 μM NaOH and further diluted in phosphate buffer containing 1% sodium dodecyl sulfate (SDS). SDS is commonly-used as a chaotropic agent; however, it can be used to stabilize amyloid oligomers by producing a membrane-like environment. NMR structure of hIAPP bound to SDS micelles revealed a predominant α-helical structure rather than the distinctive amyloidal fibrilar β-sheet[36]. Ramamoorthy and coworkers have also shown that hIAPP has an overall kinked helix motif when bound to SDS micelles in physiological pH, with residues 7–17 and 21–28 in a helical conformation, as well as a 3_{10} helix from residues 33–35[37], Several groups have independently demonstrated that hIAPP undergoes a transition from its natively disordered monomeric state to α-helical structure when interacting to membranes[38,39]. In addition, X-ray crystallography study has shown that in the crystal structure of an MBP-IAPP fusion, IAPP adopts an ordered, helical conformation[40]. All of this data suggest that SDS can be used to stabilize soluble genuine conformations of hIAPP. The peptide was further diluted in ultrapure water, and precipitated with ice-cold methanol/acetic acid solution in order to remove SDS, following which, the pellet was resuspended with PBS buffer.

hIAPP oligomers size determination. To determine the exact nature of the formed assemblies, we analyzed the resulting peptide species using several complementary methods. First, using SDS-PAGE analysis, we observed three major assembly species: Monomers of ~3.9 kDa, dimers of ~8 kDa and trimers of ~12 kDa (Figure 1A). As a negative control, we processed rat IAPP (rIAPP) which differs by six residues and does not self-assemble to form amyloid structures[41]. Indeed, as expected, we observed only the monomeric conformation in the case of the rIAPP (Figure 1A). Furthermore, The size distribution of the hIAPP assemblies was analyzed under more "native" conditions using analytic-fast liquid chromatography (FPLC) performed under physiological-like ionic strength and pH (PBS pH 7.4). Samples were loaded on a size-exclusion column and the size distribution of the species was determined using a calibration curve. Here again, we observed the three species previously detected in the gel analysis, as well as additional specie of ~90 kDa. This additional conformer is probably not stable in SDS-PAGE and disassembles to smaller multimers. The chromatography did not reveal evidence for larger assemblies suggesting that amyloid fibrils or larger supramolecular structures were not formed (Figure 1C). Ramamoorthy and coworkers have demonstrated in a DOSY NMR study, that hIAPP but not rIAPP forms large oligomers that do not trigger the nucleation-dependent aggregation of IAPP at 4°C, which may reflect an off-pathway intermediate as observed here[42].

hIAPP oligomers stability. Next the oligomeric structures of hIAPP, once assembled, were examined using Thioflavin T (ThT) binding assay to assess their stability and compared to hIAPP solubilized by PBS buffer. IAPP oligomers did not exhibit an increase in ThT fluorescent signal for over ten hours indicating relatively stable conformers while the control group showed a lag-phase of around four hours followed by exponential increase in the fluorescent signal (Figure 1B).

hIAPP oligomers have spherical morphology. The morphology of the oligomers was examined using atomic force microscopy (AFM), (Figure 1D). Under these experimental conditions only the larger oligomers could be detected most likely representing the ~90 kDa assemblies observed in the size exclusion analysis. The AFM

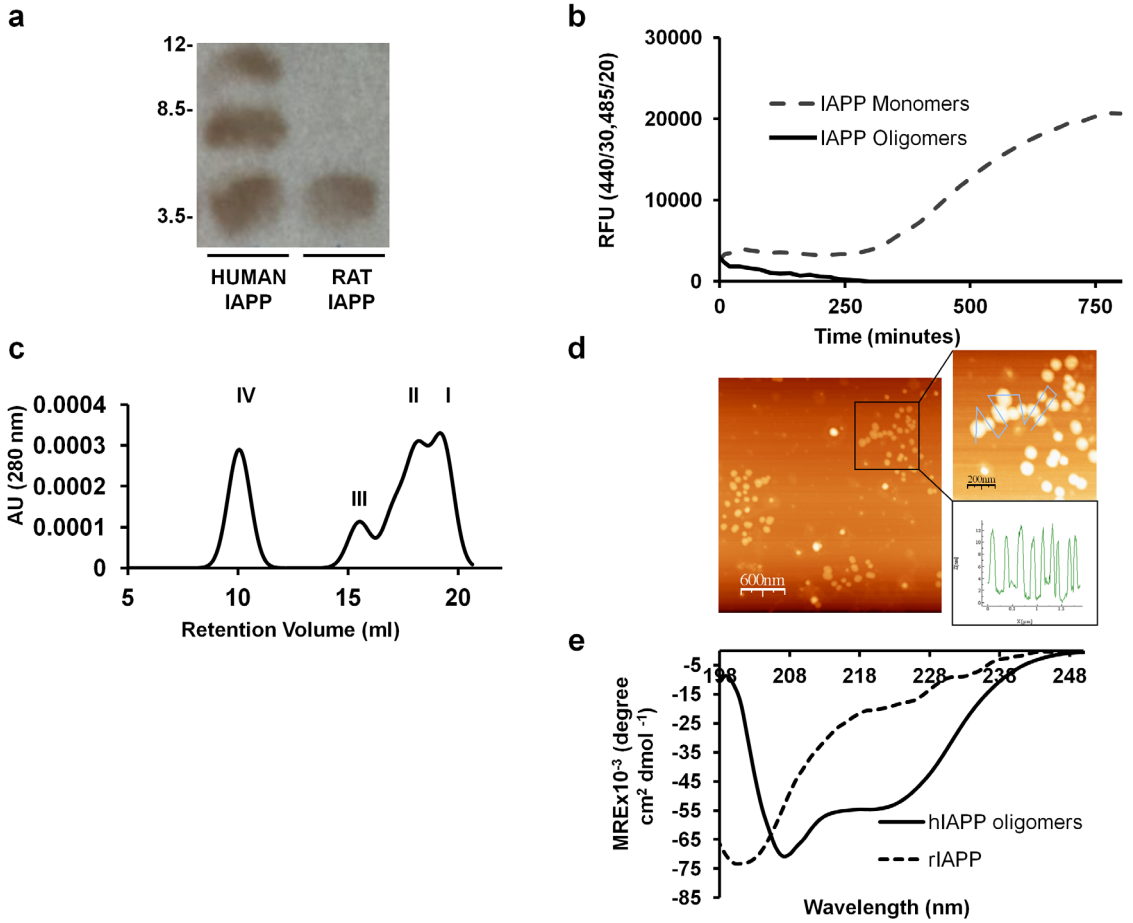

Figure 1 | Human IAPP oligomers Characterization. (a) Western-Blot analysis under non-reducing conditions of human IAPP oligomers and a negative control of non amyloidogenic rat IAPP.(b) Oligomers stability assay, hIAPP oligomers were precipitated dialyzed against PBS buffer and incubated at 37°C oligomers association was monitored by ThT analysis and compared to hIAPP dissolved in PBS buffer. (c) Size exclusion chromatography (Superdex 75 10/300, PBS buffer pH 7.4) of hIAPP oligomers; I-monomer, I-dimer, III- trimer and IV- 90 kDa oligomer. (d) Atomic force microscopy (AFM) images of the ~90 kDa oligomers, AFM scale bar 600 nm. (e) CD spectroscopy of hIAPP and rIAPP, protein concentration of 5 μM. Each spectrum represents the average of three measurements.

experiments revealed that no fibrilar aggregates were present, and the oligomers possess spherical morphology.

hIAPP oligomers are predominantly α-helical. Secondary structure analysis was performed using circular dichroism (CD) spectroscopy in the far UV (200–250 nm) (Figure 1E). The CD analysis indicated a predominant α-helical structure with two negative peaks at 222 and 208 nm. The rIAPP treated under identical conditions exhibited a significant lower α-helical content and higher random coil structures. Importantly, the CD spectrum revealed that the predominant structure is α-helical rather than β-sheet which is indicative of amyloid fiber formation appearing in the CD-spectra by a positive peak around 195 nm and a negative peak between 215–220 nm. Several studies have shown that hIAPP adopts α-helical structure upon its interaction with biological membranes[37,38], suggesting an important role of this conformation in the interaction with pancreatic β-cells.

hIAPP oligomers induce apoptosis of pancreatic β-cells. Our data indicates that the identified soluble IAPP conformers are relatively stable and possess unique physical and structural properties which differentiate them from mature amyloid fibrils. Yet, the connection to the disease etiology had to be assessed. The degree of cytotoxicity of hIAPP oligomers at different concentrations towards pancreatic RIN-m cells was evaluated by measuring mitochondrial succinate dehydrogenase activity (Figure 2A). The cell viability experiments were performed at the concentration range of 100 nM–10 μM which reflects a local concentration in which hIAPP is secreted from the granules (~400 μM). We assume that this two orders of magnitude range is relevant for the actual seeding concentration of hIAPP.

Upon the addition of hIAPP oligomers (100 nM–10 μM) the enzymatic activity declined significantly. The addition of 100 nM hIAPP oligomers resulted in a decrease of ~40% in cell viability and higher concentrations further showed a dose-dependent decreased in cell viability. Importantly, the addition of rIAPP at similar concentrations did not result in significant reduction in cell viability.

To further verify the nature of the cytotoxic activity, apoptotic and necrotic markers were analyzed using fluorescence-activated cell sorting (FACS). Pancreatic cells treated with hIAPP oligomers at various concentrations were observed to be mostly in the early and late apoptotic phases (Figure 2C). A clear and strong negative correlation between oligomers concentration and cell viability and a positive correlation to the percentage of apoptotic cells in the culture could be observed (Figure 2D).

hIAPP oligomers permeate biological membranes. hIAPP oligomers are considered to be toxic towards pancreatic cells and have been shown to induce membrane permeabilization[43,44]. To examine whether the newly identified conformers are toxic, we employed several complementary methods. As mentioned above, previous studies have demonstrated that the toxicity of different amyloid oligomers is related to the formation of discrete pores in

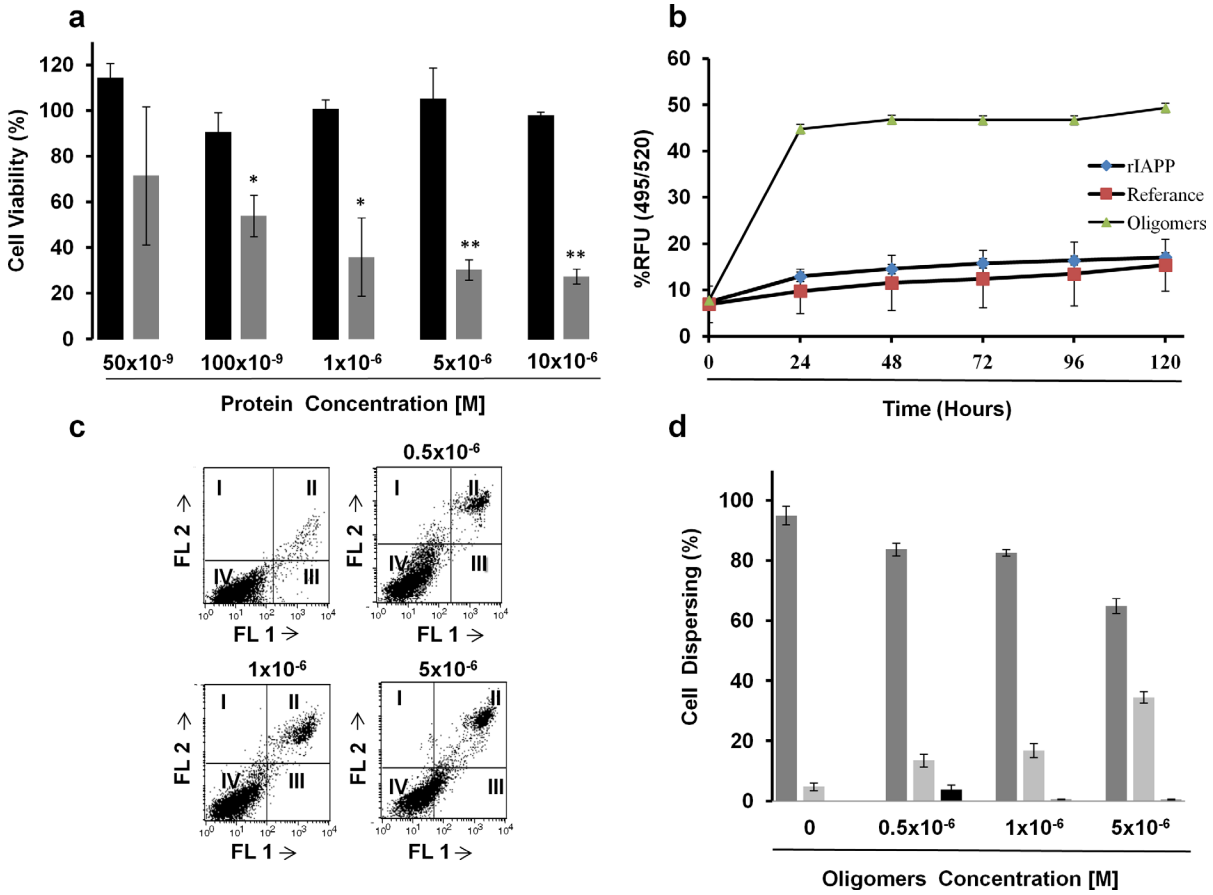

Figure 2 | Human IAPP oligomers Toxicity. (a) Rin-m cells treated with hIAPP oligomers (grey) or with rIAPP (black) in diverse concentrations. Cells viability was estimated by MTT reduction assay (*$P < 0.05$, **$P < 0.005$). (b) Dye leakage from calcein containing liposomes. 1 μM hIAPP oligomers (green rectangle) or rIAPP (blue rhombus) were incubated with the liposomes and membrane damage was evaluated by increased fluorescence (excitation: 495, emission: 520) and compared to the control group (red square). (c) FACS results of the incubation of Rin-m cells with hIAPP oligomers at different concentrations. The Annexin V-FITC apoptosis detection kit was used for the detection of apoptotic cells. FL1-H is the fluorescence of V-FITC and FL2-H is the fluorescence of Annexin V-PE. **I**-cells in necrotic state, **II**- late apoptotic state, **III**- early apoptotic state and **IV**- viable cells (d) Diagram presentation of cell state dispersion of three FACS analysis assays, as presented in figure 2C, dark grey column represent viable cells, light grey column represent early and late apoptotic cells and black column represent necrotic cells.

biological membranes[13,44,45]. To examine whether hIAPP oligomers act in a similar manner, we used a liposomal system as a cell membrane model. Liposomes were packed with a solution of concentrated calcein fluorescent dye and incubated with hIAPP oligomers (10 μM, 37°C) or rIAPP as a negative control and the fluorescence was monitored over time. Indeed, hIAPP oligomers rapidly permeabilized the liposome membrane leading to the release of the fluorescent dye to the medium while rIAPP did not exhibit any membrane damaging abilities (Figure 2B). These results indicate that amyloid fiber formation is not necessary for membrane disruption by hIAPP and suggest a direct role of the newly identified oligomers as toxic species.

Fluorescently-tagged hIAPP was used to establish physical interaction between the oligomers and β-cells. The labeled polypeptide was subjected to the same protocol as described above, resulting in the formation of identical oligomers as the unlabelled hIAPP (data not shown). Assembled labeled oligomers were incubated for different time periods with pancreatic cells and analyzed by confocal microscopy (Figure 3). After one to two hours localization of the oligomers on to the cell membrane was detected. This was followed by internalization of the oligomers into the cytoplasm which was readily observed after four hours. This was also accompanied by massive decline in cell numbers. Cell morphology changes were evident after six to eight hours. These results further underscore the cytotoxic effect of the oligomers and their specific interaction and internalization to pancreatic cells.

In order to study the cellular localization of the oligomers, live cell imaging analysis was performed. As demonstrated in figure 4, we observed co-localization of some of the oligomers in the lysosome, while the other oligomers exhibit non-localized diffusion staining along the cells. This observation is in agreement with the work of Serpell and coworkers who studied the localization of Aβ oligomers[46]. The similarly between Aβ and IAPP oligomer cellular localization further supports a common mechanism of cytotoxicity for various oligomeric assemblies.

Type 2 diabetes autoantibodies recognize the hIAPP oligomers. Next, we examined the relevance of the newly identified oligomeric structures to the etiology of the disease. In order to achieve this, we inspected whether specific antibodies that would recognize the hIAPP assemblies could be identified from T2DM patient sera. To this end, antibodies were purified from three T2DM patients and three healthy individuals and their ability to detect the hIAPP oligomers was compared. We used Dot-Blot analysis for assessing the affinity of the purified serum antibodies to the oligomers (Figure 5A). Antibodies from T2DM patients exhibit binding activity towards the oligomers at lower concentrations compared to purified antibodies from serum of healthy individuals. At a

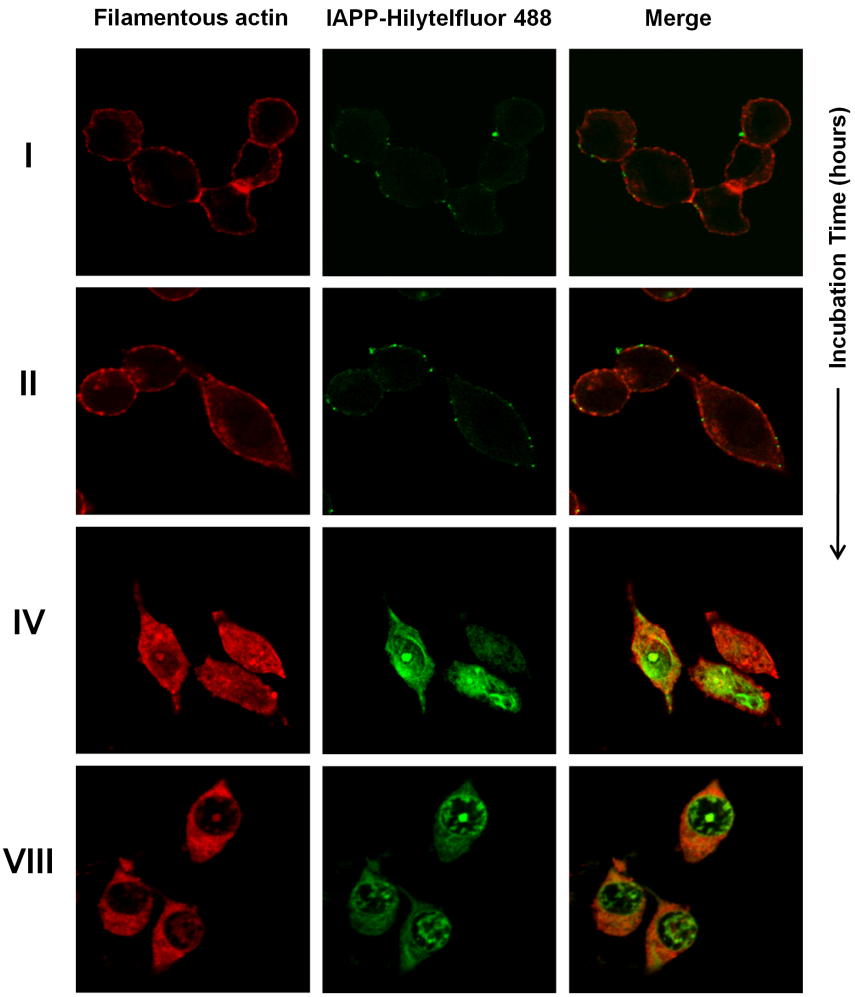

Figure 3 | hIAPP oligomers permeabilize cell membrane. Confocal microscopic images of Rin-m cells incubated with 5 μM of hIAPP-Hiytelfluor 488 oligomers, cells were stained with phalloidin–tetramethylrhodamine. Incubation was preformed for one hour (I), two hours (II), four hours (IV) and eight hours (VIII). After one hour localization of hIAPP oligomers to cells membrane was observed followed by insertion to cell cytoplasm and cell morphology alteration at longer incubation times.

concentration of 20 μg/ml antibodies purified from T2D patients displayed a higher binding activity than those purified from healthy subjects. Lower antibody concentrations showed hIAPP oligomers binding only by antibodies isolated from T2D patients emphasizing their specificity (Figure 5A). In order to further confirm these results, antibodies from new samples, ten T2DM patients and ten healthy individuals (five females and five males in each group, Table S1), were purified. Antibody recognition was assessed by Enzyme-linked immunosorbent spot (ELISPOT) assay (Figure 5B). The result clearly demonstrates the existence of antibodies that binds soluble IAPP conformers in diabetic patients but not in healthy individuals.

To examine whether hIAPP conformers recognized by antibodies from T2DM patients are indeed the oligomeric one, ELISA assay was used to evaluate the recognition of different hIAPP states (monomers, oligomers and fibrilar structures). Homogenous monomers were achieved by dissolving hIAPP in 0.2 μM NaOH after HFIP treatment and dilution with 8 M guanidinium hydrochloride solution (final guanidinium hydrochloride concentration of 7 M). Oligomers were produced by the protocol described above. Fibrilar structures were formed in PBS buffer, confirmed by ThT assay and TEM microscopy, and were centrifuged $60*10^3$ g for one hour to verify that only large aggregate are present. The pellet was resuspended in PBS buffer quantified and loaded to the ELISA plate. As shown in Figure 5D, the oligomeric species were recognized by the antibodies significantly to a higher extent as compared to the other conformers. These results suggest that hIAPP oligomers occur *in vivo* during the progress of T2DM. Together with the various experiments described above they strongly implicate a major causal role of hIAPP oligomers in the etiology of this disease.

Type 2 diabetes autoantibodies reduce the cytotoxic effect of hIAPP oligomers. We further tested whether T2DM-associated antibodies are able to reduce the cytotoxic effect of the oligomers. Notably, cells incubated both with hIAPP oligomers and patients-derived antibodies showed cell viability increase in a dose-dependent manner; up to 65% of cell viability was measured, compared to only 35% of cell viability that was measured merely with oligomers. Negative control with healthy individuals derived antibodies did not exhibit any significant change in cell viability (Figure 5C). These results further suggested that the T2DM-derived antibodies recognize specifically the oligomers and are able to reduce toxicity due to physical interaction with the toxic oligomers.

Discussion

In recent years the "amyloid hypothesis" has been challenged by evidence connecting early soluble oligomers with amyloid-related pathology. Accordingly, the study of soluble amyloidal assemblies is important both for mechanistic insights as well as for development of new therapies. Yet, the examination of such conformers is challenging,

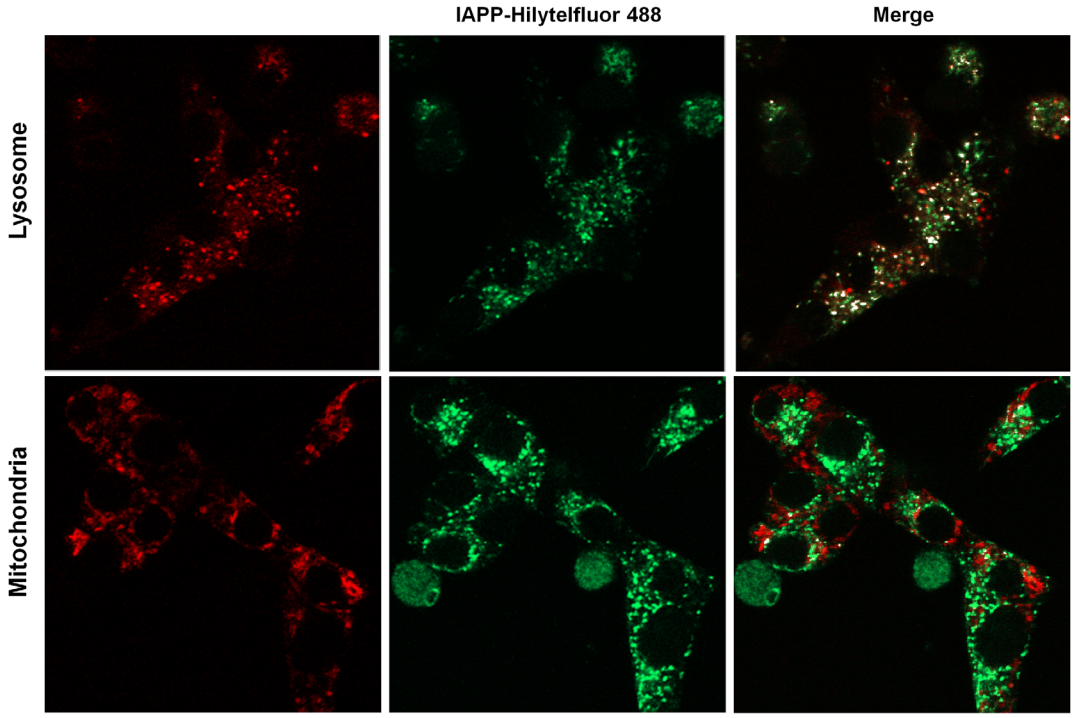

Figure 4 | hIAPP oligomers cellular localization. Live confocal microscopy images of Rin-m cells incubated 5 μM of hIAPP-Hiytelfluor 488 oligomers for 3 hours (Green), Lysosome was stained using LysoTracker reagent (red), mitochondria was stained using MitoTracker (red). As shown, some oligomers were observed to localize in the lysosome (white) while others showed a diffusion pattern along the cell.

since the amyloid self-assembly cascade is a complex network of intermolecular events resulting in the formation of pseudo-stable conformers with variable sizes[47].

Here we present an approach for production of soluble hIAPP oligomers; these oligomers remained stable for a significant time period, whereas hIAPP that was solubilized in a standard protocol rapidly aggregated, as was demonstrated by the ThT assay. Several complementary assays were applied to characterize the biophysical properties of the oligomers. The conformation of the oligomers was found to be predominantly α-helically, with two negative peaks at 222 and 208 nm. Size distribution analysis revealed four main populations: monomers, dimers, trimers and ~90 kDa oligomers; the morphology of these structures appeared mostly spherical, with no fibrilar aggregates. The spherical morphology which hIAPP oligomers adopt resembles the globular or annular appearances that were previously reported for several amyloid polypeptide oligomers, displaying a pore or ring shaped structures[14,45,48,49]. Interestingly, spherical oligomers rather than the annular oligomers were shown to increase membrane conductance and induce apoptosis in cell culture[50].

In addition, previous reports show that hIAPP adopts helical structure upon its interaction with biological membranes[51]. Gafni and coworkers reported that, hIAPP 1–19 fragment, similar to the full length peptide; adopt an α-helical conformation upon binding to lipid membranes. As opposed to the wild type sequence, the hIAPP1-19 fragment does not form amyloid fibrils even at high concentrations; at these concentrations, the fragment show a greater membrane disruption compared to the full length peptide[39]. Recently, Miranker and coworkers studied hIAPP variant (L12N/N14L), which tends to form β-sheet fibers rather than α-helical structures. Intriguingly, the hIAPP variant is significantly less toxic compare to the wild type sequence[51]. These studies emphasize the significance of studying the oligomeric alpha helical state of hIAPP and its implication on membrane damage and cell cytotoxicity. The oligomers presented here exhibited high cytotoxicity towards pancreatic cell line; a dose dependent decrease in cellular mitochondrial reductase activity and elevated apoptotic markers were observed following oligomers exposure. Moreover, using fluorescently tagged oligomers we observed localization of the oligomers on the cellular membrane after 1–2 hours, followed by internalization after ~4 hours. Longer incubation period manifested by a change in cellular morphology and reduction of viable cells. The interaction between the oligomers and biological membranes was verified using a liposomal model assay. The oligomers induced rapid membrane permeabilization, while the non aggregative rIAPP peptide did not show any effect. Our findings support previous reports demonstrating that amyloid assemblies interact with cell membranes, causing ion flux through artificial and cellular lipid membranes[52]. Furthermore, Glabe and coworkers have shown that amyloid oligomers share structural and functional homology with pore forming proteins like alpha-hemolysin from the bacterium *Staphylococcus aureus*, as well as human perforin from cytotoxic T lymphocytes[53].

To confirm the pathological relevance of the obtained conformers we screened for antibodies that recognize hIAPP assemblies. Naturally occurring auto-antibodies were previously found to target amyloid β[54] and α−synuclein[55,56]. In spite of the identification of the antibodies, clinical signs of the diseases are also observed. It is most likely that the degenerative process occurs simultaneously with the production of the antibodies, thus making it difficult to study the two phenomena separately. The production of antibodies, early in the progression of such multifactorial diseases, may suggest that a better direction for clinical intervention should be at the early stages of the diseases before permanent damage of tissues and organs is observed.

Overall, we examined 13 samples of T2DM patients and 13 samples of healthy individuals. First, we used dot-blot assay applying serial dilutions of antibodies. At a concentration of 10 μg/ml hIAPP oligomers, T2DM antibodies exhibit ~4 fold higher binding compared to antibodies of healthy individuals, while at a concentration of 5 μg/ml hIAPP oligomers, we observed only binding of T2DM. ELISPOT assay was performed to accurately quantify the antibodies binding levels. In agreement with the dot-blot assay, T2DM derived antibodies exhibited much higher binding properties than healthy individuals antibodies.

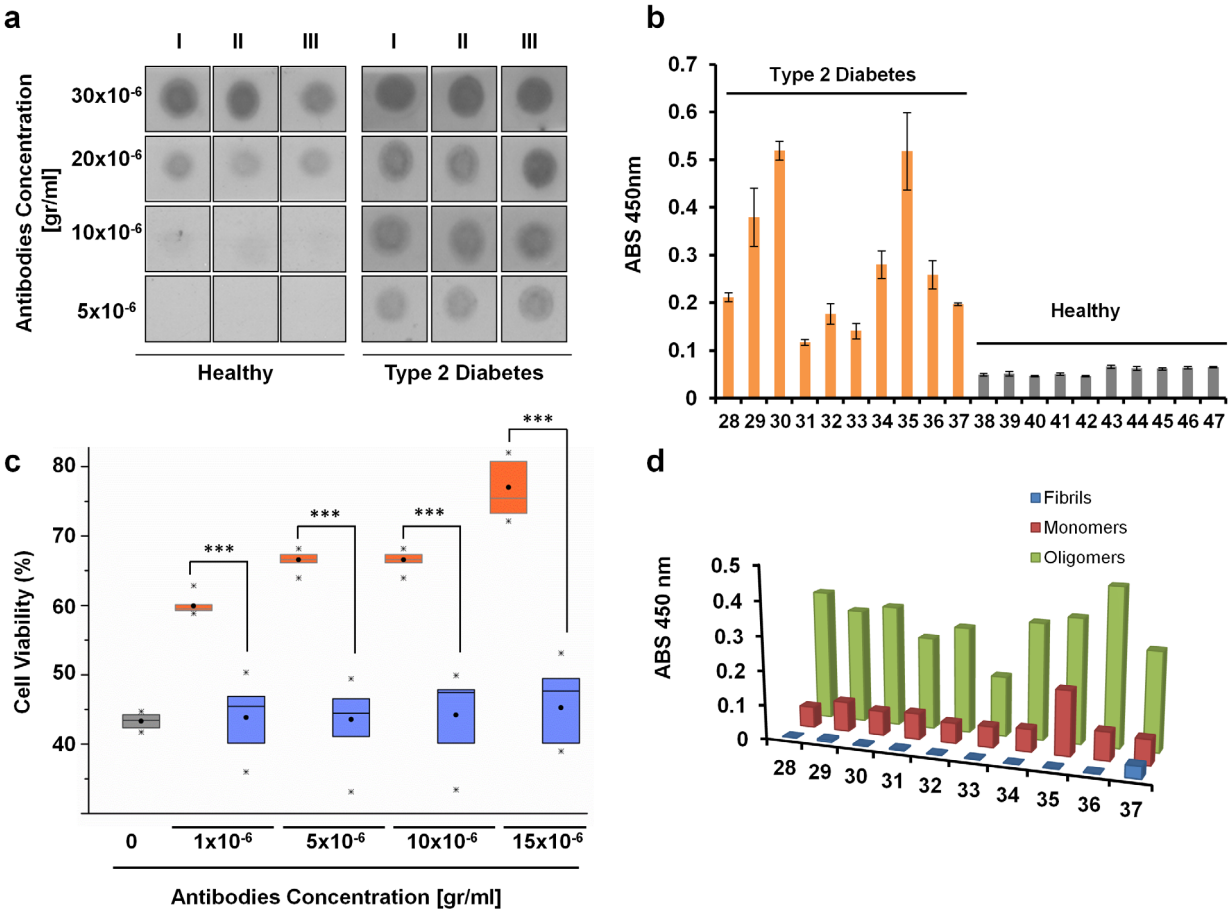

Figure 5 | Antibodies from Type 2 Diabetes patients recognize and neutralize hIAPP oligomers. (a) Purified antibodies from the serum of type 2 diabetes patients and healthy people (N = 3) was compared to the recognition of hIAPP oligomers (5 μg) by dot blot analysis through serial dilutions of purified antibodies. (b) Purified antibodies from the serum of type 2 diabetes (orange columns) and healthy people (grey columns, N = 10) recognition of hIAPP oligomers (5 μg) was compared by ELISPOT assay. (c) Rin-m cells treated with hIAPP oligomers (grey) with or without type 2 diabetes (orange) or healthy individuals (blue) purified antibodies in diverse concentration was examined for viability by MTT reduction assay and compared to the non-treated cells, Box-plots showing statistical distributions of cell viability after treatment (the box size represent the SD, black circles are the average, the horizontal line is the median and the upper and lower asterisks are 99th and 1st percentile respectively) ***P < 0.0001. (d) Type 2 diabetes antibodies recognition of different hIAPP conformers was examined by ELISPOT assay (Fibrils in blue columns, monomers in red columns and oligomers in green columns).

ELISPOT assay was also conducted with different hIAPP conformers (monomers, oligomers and fibrilar aggregates). The oligomers displayed significantly higher antigenic tendency compared to the other conformers. Finally, we examined whether the antibodies attenuate the oligomers toxicity. Indeed, the antibodies increased cell viability in a dose dependent manner, virtually doubling the viability of cells treated with hIAPP oligomers, upon addition of 15 μM of antibodies. The specificity of T2DM antibodies for oligomeric species of hIAPP and the ability of the antibodies to reduce hIAPP cytotoxicity suggest the oligomeric conformers are the major toxic element responsible for cellular apoptosis observed in the pancreas during IAPP self-assembly.

We tried to diversify the tested samples as much as we could, half are men and half are women, in the healthy group the youngest is 22 and the oldest is 48, at the T2DM group the range is 40 to 74 (Table S1). The diagnosis time also varied from 1998 to 2010, we did observe a variance between the samples, at this point we cannot link any variable to the antibodies titer, an extensive screen is needed to examine the correlation between antibodies appearance and the disease progression, also to determine the different factors that influence the antibody titer.

Our results provide clear evidence for the role of the oligomeric species, rather than the monomeric form of IAPP, in the pathological cascade that results in cell death and loss of pancreatic β-cell mass. It was demonstrated that the oligomeric assemblies induce apoptotic cell death likely by their interaction with the cell membrane. The ability of antibodies from human patients to interact specifically with hIAPP oligomers suggests that the formed assemblies as described here represent valid epitopes present in diabetic patients. Moreover, the ability of these antibodies to annul the toxic activity of the oligomeric species paves the way for new therapeutic approaches for the treatment of β-cell mass loss in the advanced stage of T2DM. The newly indentified and characterized species could serve as epitopes for the development of immune response in active or passive immunization. Furthermore, these species could serve as a facile platform for screening and optimizing compounds which are able to interfere with the toxic effect of oligomeric species.

Methods

Oligomers preparation. IAPP synthetic peptide (Human; H-7905, Bachem, Bubendorf, Switzerland. Rat; 74-5-10A, American peptide, California, U.S.A) was dissolved in 100% HFIP, 1 mg/ml and incubated for complete solubilization under shaking (100 rpm) at 37°C for 2 h. HFIP was removed by Speedvac apparatus (Eppendorf, Germany), the peptide was resuspended in 0.2 μM NaOH to a final concentration of 5 mM and sonicated for 2 minutes in a pre-chilled sonication bath to insure complete solubilization. The peptide preparation was diluted in phosphate-buffered saline (PBS, 10 mM pH 7.4) with 1% SDS to a final concentration of 600 μM and incubated for 4–7 hours at 37°C. The peptide preparation was further diluted in ultra pure H_2O to a final concentration of 200 μM and incubated for 12 Hours, 37°C. IAPP self- assembly products were analyzed by 15% Tris-tricine PAGE and stained

with Imperial protein stain. Oligomers were precipitated by a nine fold excess (v/v) of ice-cold methanol/acetic acid solution (33% methanol, 4% acetic acid) for 1 h at 4°C. The oligomers was then pelleted (10 min at 16,200 g), resuspended in PBS buffer (10 mM pH 7.4). In order to make sure SDS is removed entirely, samples were dialyzed against PBS buffer over night at 4°C. IAPP oligomers were examined after treatment by PAGE analysis and Size exclusion chromatography and shown no change in size distribution.

Size exclusion chromatography. IAPP oligomers was prepared as mentioned above (0.1 mg, 200 μM) were loaded on Superdex 75 column 10/300 (Amersham Biosciences, Sweden), 0.5 ml/min, PBS buffer. Size was determined using a calibration curve calculated with 5 protein standard (Bio-Rad. USA). Peaks Deconvolution was calculated by PeakFit software (SYSTAT software Inc.).

ThT binding fluorescence. IAPP oligomers were prepared as mentioned above, after precipitation with ice-cold methanol/acetic acid solution and dialysis against PBS buffer, oligomers aggregation was compared to hIAPP peptide dissolved in 0.2 μM NaOH (5 mM) and further diluted in PBS buffer (10 mM pH 7.4, peptide concentration 10 μM). ThT (Sigma) was dissolved in PBS buffer and filtered with 0.22-μM filter. ThT (1 μM) was added to each sample (10 μM) and aggregation was monitored over time by Biotek Synergy plate reader (Biotek) measurement of each data point at an interval of 5 min, 37°C.

Atomic force microscopy. AFM analysis was generated by depositing an aliquot of 40 μl (concentration of 200 μM) on a freshly cleaved mica surface. Samples were probed by a Digital Instrument (DI) MultiMode™ NanoScope IV AFM, using a Mikromasch NSC15/Si3N4 cantilever (resonant frequency $f = 325$ kHz, spring constant $k = 40$ N/m) in a tapping mode.

Circular dichroism (CD) spectroscopy. CD spectra were obtained using an AVIV 202 spectropolarimeter equipped with a temperature-controlled sample holder and a 10 mm path length cuvette. All experiments were performed in PBS, pH 7.4, peptides concentration of 5 μM. For wavelength scan experiments, each spectrum represents the average of three scans. Evaluation of the secondary structure composition obtained from far-UV CD spectra was facilitated by using the K2d and CDNN software.

Liposomes membrane damage measurements. Phosphatidyl ethanolamine, phosphatidyl serine and phosphatidyl choline (Avanti, USA) were dissolved in chloroform at a concentration of 20 mg/ml in a molar ratio of 5 : 3 : 2 respectively. Solvent was removed from sample by evaporating the chloroform under a stream of nitrogen gas in a rotor vapor apparatus to deposit a thin lipid film on the walls of a glass test tube. The dry lipid film was then rehydrated in the 50 mM sodium phosphate buffer (pH 7.4) containing 40 mM sodium calcein to make multilamellar vesicles (MLVs) at a concentration of 40 mg/ml. The MLVs were then subjected to several sonication cycles to equilibrate the vesicles with the buffer. Nonencapsulated calcein was removed from vesicles through size exclusion chromatography using a HiPrep 16/60 sephacryl S-100 column (Amersham Pharmacia Biotech, Uppsala, Sweden).packed vesicles with calcein were confirmed by fluorescent measurements before and after adding 1% of triton x-100. Samples were incubated at 37°C and the membrane damage rate was followed by Fluorescence assay (excitation at 495 nm, 2.5 nm slit, and emission at 520 nm, 5 nm slit). Measurements were taken using a Jobin Yvon Horiba Fluoromax-3 fluorimeter (Horiba, Japan). Each point represents the average of three independent measurements.

MTT reduction assay. Rin-m cells (2×10^5 cells/ml) were cultured in 96-well micro plates (100 μl/well) and incubated overnight at 37°C. Human oligomers and rat IAPP were added to each well at various concentrations and incubated for 6 hours at 37°C. Following incubation cell viability was evaluated using 3-(4, 5-dimethylthiazolyl-2)-2, 5-diphenyltetrazolium bromide (MTT) assay. Briefly, 20 μL of 5 mg/ml MTT dissolved in PBS was added to each well. After 4 hours incubation at 37°C, 100 μl of extraction buffer [20% SDS dissolved in a solution of 50% dimethylformamide and 50% DDW (pH 4.7)] was added to each well, and the plates were incubated again overnight at 37°C. Finally, color intensity was measured using an ELISA plate reader at 570 nm and background subtraction at 650 nm.

Flow cytometry cell sorting (FACS) assay. Rin-m cells (5×10^5 cells/ml) were cultured for 4 hours at 37°C incubated with human IAPP oligomers (final concentration of 0.5 μM, 1 μM and 5 μM). Samples were washed with PBS buffer and resuspended with 500 μl binding buffer. Samples were added 5 μl of Annexin V-FITC and 10 μl of propidium iodide (Annexin V-FITC apoptosis detection kit; MBL). After 10 minutes of incubation in the dark at room temperature, samples were analyzed using the FACS Sort (Beckton Dickinson) and results analyzed using the CellQuest program (Beckton Dickinson). Each measurement was repeated three times. FL1-H represents the fluorescence of Annexin V-FITC and FL2-H represents the fluorescence of propidium iodide.

Confocal microscopy. Rin-m cells were cultured on glass cover-slip placed in 24-well micro plates, then incubated for different periods with fluorescent tagged hIAPP Oligomers (5 μM) at 37°C, as described in the cell cytotoxicity experiments section. hIAPP was tagged with Lys(Hilytefluor 488)-NH2 at the C-terminal end (Anaspec, USA). After incubation cells were washed with PBS buffer and fixed with 4% paraformaldehyde in PBS for 5 minutes and washed with PBS buffer. Cells were treated with 1% Triton x-100 in PBS and stained with 50 μg/ml Phalloidin Tetramethyl-rhodamine B isothiocyanate (Sigma-Aldrich) in PBS, 40 minutes in room temperature, followed by extensive wash with PBS buffer. The cells were imaged using LSM 510 confocal laser scanning microscope (Carl Zeiss Jena, Germany). For the cell Live imaging experiment Rin-m cells were cultured on a cell culture dish with a glass bottom (35 mm, greiner bio-one) and incubated with hIAPP-Hilytefluor 488 oligomers for 3 hours, the mitochondria was stained with MitoTracker® Red reagent (molecular probes) according the manufacture instructions for 1 hour (100 nM). Cell lysosomes were stained using LysoTracker® Red DND-99 (molecular probes) according the manufacture instructions for 1 hour (50 nM). Images were acquired using LSM 510 Meta confocal laser scanning microscope (Carl Zeiss Jena, Germany).

Antibodies purification. Antibodies from healthy and type 2 diabetes patients' serum (Bioreclamation, USA) were purified by protein-A column (GE healthcare). 1 ml of Human Serum was diluted 1 : 20 with loading buffer (20 mM Na_2HPO_4, 2 mM NaH_2PO_4 pH 7) and loaded onto a 5-ml protein-A column, flow throw was collected and reloaded 3 times. Bound antibody was eluted with 0.1 M of citric acid (pH 3.0) and neutralized with 1 M Tris-HCl (pH 9.0) for 1 ml of eluate 200 μl of Tris buffer was added. Protein-containing fractions were combined, dialyzed against 2 liter PBS buffer (16 h, 4°C). Antibodies concentration was determined using Bradford reagent (Sigma-Aldrich). Antibody purity was assessed by SDS-Page.

Antibodies recognition assays. Antibodies recognition was evaluated by Dot-blot and ELISA assay. For the Dot-blot experiments hIAPP oligomers (5 μg) were spotted onto a nitrocellulose membrane via a vacuum manifold. After blocking the membrane with 5% skim milk in TBS-T (50 mM tris, 150 mM NaCl pH = 7.5 with 0.3% tween 20) for 1 hour at room temperature. Membrane was washed briefly with TBS and incubated with purified antibodies at several concentrations for 2 hours, room temperature. Then, membrane was washed briefly with TBS-T and incubated with HRP-conjugated donkey anti-human HRP antibody (Jackson immunoResearch laboratories, USA). The membrane was developed using ECL reagents (NEN, USA) according to the supplier's instructions. Positive control with rabbit anti-IAPP antibody (Santa Cruz Biotechnology, USA) was preformed. ELISPOT assay was done by adsorbing hIAPP oligomers (5 μg) onto the wells of a BioTrace PVDF Membrane 96-well plate (PALL, USA), 3 hours room temperature. Wells were blocked with 3% bovine serum albumin (BSA) in TBS-T for 1 hour at room temperature, the plate was washed briefly with TBS and incubated with purified antibodies (10 μg/ml) for 2 hours, room temperature. The plate was washed extensively with TBS-T and incubated with HRP-conjugated donkey anti human HRP antibody (Jackson immunoResearch laboratories, USA). Binding was quantified by 3,3′,5,5′-tetramethylbenzidine reagent (TMB, Pierce) according to the manufacture instruction.

In order to examine which of the assemblies T2DM antibodies recognize. ELISA assay was also used to compare the T2DM antibodies (10 μg/ml) recognition toward different hIAPP conformers as explained above, Fibrillar structures were formed by dissolving hIAPP in 0.2 μM NaOH after HFIP treatment and dilution with PBS buffer (peptide concentration 10 μM), peptide was incubated for 48 hours in 37°C, centrifuged 60,000 g for 1 hour to confirm only large aggregate are present. The pellet was resuspended in PBS buffer and quantified by Bradford reagent (Sigma-Aldrich), Homogenous monomers were achieved by dissolving hIAPP in 0.2 μM NaOH after HFIP treatment and dilution with 8 M Guanidinium chloride solution (final Guanidinium chloride concentration of 7 M, peptide concentration 10 μM).

Antibodies neutralizing effect. Rin-m cells (2×10^5 cells/ml) were cultured in 96-well micro plates (100 μl/well) and incubated overnight at 37°C. Human oligomers (5 μM) with or without antibodies was added to each well at various concentrations. Each measurement was repeated four times; also, a control measurement with antibodies alone at the highest concentration was preformed to refute any effect of antibodies on cell viability. Following incubation for 6 hours at 37°C, cell viability was evaluated using 3-(4, 5-dimethylthiazolyl-2)-2, 5-diphenyltetrazolium bromide (MTT) assay as described above.

Statistical analysis. Quantitative results are shown as means ± SD. The statistical analysis was performed by Student's t test between control and tested groups. P value of ≤ 0.05 was considered significant. *, Pv ≤ 0.05, **, Pv ≤ 0.005 and ***, Pv ≤ 0.005.

1. Eisenberg, D. & Jucker, M. The amyloid state of proteins in human diseases. *Cell* **148**, 1188–1203 (2012).
2. Haass, C. The molecular significance of amyloid beta-peptide for Alzheimer's disease. *Eur. Arch. Psychiatry Clin. Neurosci.* **246**, 118–123 (1996).
3. Conway, K. A., Harper, J. D. & Lansbury, P. T. Accelerated in vitro fibril formation by a mutant alpha-synuclein linked to early-onset Parkinson disease. *Nat. Med.* **4**, 1318–1320 (1998).
4. Chuang, L. M. *et al*. Role of S20G mutation of amylin gene in insulin secretion, insulin sensitivity, and type 2 diabetes mellitus in Taiwanese patients. *Diabetologia.* **41**, 1250–1251 (1998).
5. Terry, R. D. *et al*. Physical basis of cognitive alterations in alzheimer's disease: Synapse loss is the major correlate of cognitive impairment. *Annals of Neurology.* **30**, 572–580 (1991).

6. Dickson, D. W. *et al.* Identification of normal and pathological aging in prospectively studied nondemented elderly humans. *Neurobiol. Aging.* **13**, 179–189 (1992).
7. Snowdon, D. A. Aging and Alzheimer's disease: lessons from the Nun Study. *Gerontologist* **37**, 150–156 (1997).
8. Bucciantini, M. *et al.* Inherent toxicity of aggregates implies a common mechanism for protein misfolding diseases. *Nature* **416**, 507–511 (2002).
9. Lambert, M. P. *et al.* Diffusible, nonfibrillar ligands derived from Aβ1-42 are potent central nervous system neurotoxins. *Proc. Natl. Acad. Sci. U. S. A.* **95**, 6448–6453 (1998).
10. Dahlgren, K. N. *et al.* Oligomeric and fibrillar species of amyloid-beta peptides differentially affect neuronal viability. *J. Biol. Chem.* **277**, 32046–32053 (2002).
11. Walsh, D. M. *et al.* Naturally secreted oligomers of amyloid beta protein potently inhibit hippocampal long-term potentiation in vivo. *Nature* **416**, 535–539 (2002).
12. Quist, A. *et al.* Amyloid ion channels: a common structural link for protein-misfolding disease. *Proc. Natl. Acad. Sci. U. S. A.* **102**, 10427–10432 (2005).
13. Bucciantini, M. *et al.* Prefibrillar amyloid protein aggregates share common features of cytotoxicity. *J. Biol. Chem.* **279**, 31374–31382 (2004).
14. Sciacca, M. F. *et al.* Two-step mechanism of membrane disruption by Aβ through membrane fragmentation and pore formation. *Biophys. J.* **103**, 702–710 (2012).
15. Kayed, R. *et al.* Common structure of soluble amyloid oligomers implies common mechanism of pathogenesis. *Science* **300**, 486–489 (2003).
16. Opie, E. L. On the relation of chronic interstitial pancreatitis to the islands of Langerhans and to diabetes melutus. *J. Exp. Med.* **5**, 397–428 (1901).
17. SE, W. A. Zur Kenntnis der feineren Veränderungen des Pankreas bei Diabetes mellitus. *Wien. Klin. Wochenshr.* **14**, 968–972 (1901).
18. Bell, E. T. Hyalinization of the islets of Langerhans in nondiabetic individuals. *Am. J. Pathol.* **35**, 801–805 (1959).
19. Westermark, P. Mast cells in the islets of Langerhans in insular amyloidosis. *Virchows Arch. A Pathol. Pathol. Anat.* **354**, 17–23 (1971).
20. Westermark, P., Wernstedt, C., Wilander, E. & Sletten, K. A novel peptide in the calcitonin gene related peptide family as an amyloid fibril protein in the endocrine pancreas. *Biochem. Biophys. Res. Commun.* **140**, 827–831 (1986).
21. Westermark, P. *et al.* Amyloid fibrils in human insulinoma and islets of Langerhans of the diabetic cat are derived from a neuropeptide-like protein also present in normal islet cells. *Proc. Natl. Acad. Sci. U. S. A.* **84**, 3881–3885 (1987).
22. Westermark, P., Wernstedt, C., O'Brien, T. D., Hayden, D. W. & Johnson, K. H. Islet amyloid in type 2 human diabetes mellitus and adult diabetic cats contains a novel putative polypeptide hormone. *Am. J. Pathol.* **127**, 414–417 (1987).
23. Cooper, G. J. *et al.* Amylin found in amyloid deposits in human type 2 diabetes mellitus may be a hormone that regulates glycogen metabolism in skeletal muscle. *Proc. Natl. Acad. Sci. U. S. A.* **85**, 7763–7766 (1988).
24. Westermark, P. & Grimelius, L. The pancreatic islet cells in insular amyloidosis in human diabetic and non-diabetic adults. *Acta Pathol. Microbiol. Scand. A* **81**, 291–300 (1973).
25. Westermark, P. & Wilander, E. The influence of amyloid deposits on the islet volume in maturity onset diabetes mellitus. *Diabetologia* **15**, 417–421 (1978).
26. Röcken, C., Linke, R. & Saeger, W. Immunohistology of islet amyloid polypeptide in diabetes mellitus: Semi-qantitative studies in a post-mortem series. *Virchows Archiv. A* **421**, 339–344 (1992).
27. Sakagashira, S. *et al.* S20G Mutant amylin exhibits increased in vitro amyloidogenicity and increased intracellular cytotoxicity compared to wild-type amylin. *Am. J. Pathol.* **157**, 2101–2109 (2000).
28. Lorenzo, A., Razzaboni, B., Weir, G. C. & Yankner, B. A. Pancreatic islet cell toxicity of amylin associated with type-2 diabetes mellitus. *Nature* **368**, 756–760 (1994).
29. Westermark, P., Wilander, E., Westermark, G. T. & Johnson, K. H. Islet amyloid polypeptide-like immunoreactivity in the islet B cells of Type 2 (non-insulin-dependent) diabetic and non-diabetic individuals. *Diabetologia* **30**, 887–892 (1987).
30. Westermark, P. Fine structure of islets of Langerhans in insular amyloidosis. *Virchows Archiv. A* **359**, 1–18 (1973).
31. Janson, J. *et al.* Spontaneous diabetes mellitus in transgenic mice expressing human islet amyloid polypeptide. *Proc. Natl. Acad. Sci. U. S. A.* **93**, 7283–7288 (1996).
32. Butler, A. E., Janson, J., Soeller, W. C. & Butler, P. C. Increased β-cell apoptosis prevents adaptive increase in β-cell mass in mouse model of Type 2 diabetes: Evidence for role of islet amyloid formation rather than direct action of amyloid. *Diabetes* **52**, 2304–2314 (2003).
33. Janson, J., Ashley, R. H., Harrison, D., McIntyre, S. & Butler, P. C. The mechanism of islet amyloid polypeptide toxicity is membrane disruption by intermediate-sized toxic amyloid particles. *Diabetes* **48**, 491–498 (1999).
34. Dinarello, C. A., Donath, M. Y. & Mandrup-Poulsen, T. Role of IL-1β in type 2 diabetes. *Curr. Opin. Endocrinol. Diabetes. Obes.* **17**, 314–321 (2010).
35. Masters, S. L. *et al.* Activation of the NLRP3 inflammasome by islet amyloid polypeptide provides a mechanism for enhanced IL-1beta in type 2 diabetes. *Nat. Immunol.* **11**, 897–904 (2010).
36. Patil, S. M., Xu, S., Sheftic, S. R. & Alexandrescu, A. T. Dynamic alpha-helix structure of micelle-bound human amylin. *J. Biol. Chem.* **284**, 11982–11991 (2009).
37. Nanga, R. P. R., Brender, J. R., Vivekanandan, S. & Ramamoorthy, A. Structure and membrane orientation of IAPP in its natively amidated form at physiological pH in a membrane environment. *Biochim. Biophys. Acta* **1808**, 2337–2342 (2011).
38. Apostolidou, M., Jayasinghe, S. A. & Langen, R. Structure of alpha-helical membrane-bound human islet amyloid polypeptide and its implications for membrane-mediated misfolding. *J. Biol. Chem.* **283**, 17205–17210 (2008).
39. Brender, J. R. *et al.* Amyloid fiber formation and membrane disruption are separate processes localized in two distinct regions of IAPP, the type-2-diabetes-related peptide. *J. Am. Chem. Soc.* **130**, 6424–6429 (2008).
40. Wiltzius, J. J., Sievers, S. A., Sawaya, M. R. & Eisenberg, D. Atomic structures of IAPP (amylin) fusions suggest a mechanism for fibrillation and the role of insulin in the process. *Protein Sci.* **18**, 1521–1530 (2009).
41. Westermark, P., Engstrom, U., Johnson, K. H., Westermark, G. T. & Betsholtz, C. Islet amyloid polypeptide: pinpointing amino acid residues linked to amyloid fibril formation. *Proc. Natl. Acad. Sci. U. S. A.* **87**, 5036–5040 (1990).
42. Nanga, R. P. R., Brender, J. R., Xu, J., Veglia, G. & Ramamoorthy, A. Structures of rat and human islet amyloid polypeptide IAPP1−19 in micelles by NMR spectroscopy. *Biochemistry* **47**, 12689–12697 (2008).
43. Mirzabekov, T. A., Lin, M. C. & Kagan, B. L. Pore formation by the cytotoxic islet amyloid peptide amylin. *J. Biol. Chem.* **271**, 1988–1992 (1996).
44. Last, N. B. & Miranker, A. D. Common mechanism unites membrane poration by amyloid and antimicrobial peptides. *Proc. Natl. Acad. Sci. U. S. A.* **110**, 6382–6387 (2013).
45. Volles, M. J. & Lansbury, P. T. Vesicle permeabilization by protofibrillar α-Synuclein is sensitive to Parkinson's disease-linked mutations and occurs by a pore-like mechanism. *Biochemistry* **41**, 4595–4602 (2002).
46. Soura, V. *et al.* Visualization of co-localization in Aβ42-administered neuroblastoma cells reveals lysosome damage and autophagosome accumulation related to cell death. *Biochem. J.* **441**, 579–590 (2012).
47. Fandrich, M., Meinhardt, J. & Grigorieff, N. Structural polymorphism of Alzheimer Abeta and other amyloid fibrils. *Prion* **3**, 89–93 (2009).
48. Conway, K. A. *et al.* Acceleration of oligomerization, not fibrillization, is a shared property of both α-synuclein mutations linked to early-onset Parkinson's disease: Implications for pathogenesis and therapy. *Proc. Natl. Acad. Sci. U. S. A.* **97**, 571–576 (2000).
49. Lashuel, H. A., Hartley, D., Petre, B. M., Walz, T. & Lansbury, P. T., Jr. Neurodegenerative disease: amyloid pores from pathogenic mutations. *Nature* **418**, 291 (2002).
50. Kayed, R. *et al.* Annular protofibrils are a structurally and functionally distinct type of amyloid oligomer. *J. Biol. Chem.* **284**, 4230–4237 (2009).
51. Magzoub, M. & Miranker, A. D. Concentration-dependent transitions govern the subcellular localization of islet amyloid polypeptide. *FASEB J.* **26**, 1228–1238 (2012).
52. Demuro, A. *et al.* Calcium Dysregulation and Membrane Disruption as a Ubiquitous Neurotoxic Mechanism of Soluble Amyloid Oligomers. *J. Biol. Chem.* **280**, 17294–17300 (2005).
53. Yoshiike, Y., Kayed, R., Milton, S. C., Takashima, A. & Glabe, C. G. Pore-forming proteins share structural and functional homology with amyloid oligomers. *Neuromolecular Med.* **9**, 270–275 (2007).
54. Kellner, A. *et al.* Autoantibodies against beta-amyloid are common in Alzheimer's disease and help control plaque burden. *Ann. Neurol.* **65**, 24–31 (2009).
55. Papachroni, K. K. *et al.* Autoantibodies to alpha-synuclein in inherited Parkinson's disease. *J. Neurochem.* **101**, 749–756 (2007).
56. Yanamandra, K. *et al.* Alpha-synuclein Reactive antibodies as diagnostic biomarkers in blood sera of Parkinson's disease patients. *PLoS ONE.* **6**, e18513 (2011).

Acknowledgments

This work was supported by the Israel Science Foundation (ISF), 449/11 and the Deutsch-Israelische Projektkooperation (DIP) Program. We thank Prof. Daniel Segal, Ayala Lampel, Aviad Levin and Dr. Lihi Adler-Abramovich for their helpful insights and manuscript revision. Furthermore, we would like thank the Gazit and Segal laboratories for helpful discussions and comments.

Author contributions

Study concept and design: E.G., Y.B., S.G. and A.F.M. Acquisition of data: Y.B., I.Y., A.A., N.A. and R.S. Drafting the manuscript and critical revision: E.G., Y.B., A.F.M. and R.S. All the authors have approved the final version of the paper.

Additional information

Supplementary information accompanies this paper at http://www.nature.com/scientificreports

Competing financial interests: The authors declare no competing financial interests.

How to cite this article: Bram, Y. *et al.* Apoptosis induced by islet amyloid polypeptide soluble oligomers is neutralized by diabetes-associated specific antibodies. *Sci. Rep.* **4**, 4267; DOI:10.1038/srep04267 (2014).